

Atomic Fermi gas in the trimerized Kagomé lattice at the filling 2/3

B. Damski^{1,2}, H.-U. Everts¹, A. Honecker³, H. Fehrmann¹, L. Santos⁴ and M. Lewenstein¹

(1) Institut für Theoretische Physik, Universität Hannover, Appelstr. 2, D-30167 Hannover

(2) Instytut Fizyki, Uniwersytet Jagielloński, Reymonta 4, PL-30-059 Kraków

(3) Institut für Theoretische Physik, TU Braunschweig, Mendelssohnstr. 3, D-38106 Braunschweig

(4) Institut für Theoretische Physik III, Universität Stuttgart, Pfaffenwaldring 57 V, D-70550 Stuttgart

We study low temperature properties of an atomic spinless interacting Fermi gas in the trimerized Kagomé lattice for the case of two fermions per trimer. The system is described by a quantum spin 1/2 model on the triangular lattice with couplings depending on bonds directions. Using exact diagonalizations we show that the system exhibits non-standard properties of a *quantum spin liquid-crystal*, combining a planar antiferromagnetic order with an exceptionally large number of low energy excitations.

PACS numbers: 03.75.Ss, 05.30.Fk

One of the most fascinating recent trends in the physics of ultracold gases concerns atomic gases in optical lattices, where strongly correlated systems may be realized. Such systems offer an "atomic Hubbard toolbox" [1] to simulate various sorts of Hubbard models, and to study phenomena known in condensed matter physics in an unprecedentedly controlled manner. To name just few examples, atomic lattice gases may serve to study various spin models [2], to simulate high T_c superconductivity [3], to investigate a variety of quantum disordered systems [4], or to process quantum information [5]. Seminal experiments of Ref. [6] have stimulated a great interest in experimental studies of atomic lattice gases (cf. [7]).

Particularly fascinating in this context is the possibility of studying quantum frustrated antiferromagnets, which lie at the heart of modern quantum magnetism [8]. Recently we have proposed how to create ideal and trimerized Kagomé optical lattices, and have studied physics of various quantum gases in such lattices [9]. A Fermi-Fermi mixture with half filling for both species in the limit of strong interspecies coupling behaves as a spin 1/2 Heisenberg antiferromagnet. Such a system (having so far no analogy among solid state systems) is a paradigmatic example of a quantum spin liquid of type II [8].

In Ref. [9] we have also discussed shortly an interesting case of interacting spinless Fermi gas in the trimerized Kagomé lattice at filling 2/3 (2 atoms per trimer). Such a system behaves as a quantum magnet on the triangular lattice with couplings that depend on bond directions. In this Letter we study low temperature physics of this system using exact diagonalizations of the Hamiltonian for 12 \cdots 24 spins. We show that in the case of effective ferromagnetic couplings the system exhibits, in contrast to the semiclassical results, non-standard properties of a *quantum spin liquid-crystal*, combining a planar antiferromagnetic order with an exceptionally large number of low energy excitations, and small (if any) gap. For the effectively antiferromagnetic coupling semi-classical analysis agrees well with quantum calculations, and indicates

antiferromagnetic planar order and gapped spectrum.

The experimental realization of the considered system requires a creation of trimerized Kagomé lattice, using superlattice techniques as shown in Ref. [9]. The spinless interacting Fermi gas can then be formed, for instance, in a Bose-Fermi mixture, in the strong coupling limit, when bosons form a Mott insulator, and fermions together with 0, 1, ... bosons (bosonic holes) form fermionic composites [10]. Alternatively, one could use a gas of polarized ultracold dipolar fermions, that interact via repulsive dipolar potential decaying as the third power of the distance.

The spinless interacting Fermi gas in the trimerized Kagomé lattice is described by the extended Fermi-Hubbard Hamiltonian

$$H_{\text{FH}} = - \sum_{\langle ab \rangle} (t_{ab} f_a^\dagger f_b + \text{h.c.}) + \sum_{\langle ab \rangle} U_{ab} n_a n_b,$$

where $a = \{\alpha, i\}$ with α referring to intra-trimer indices and i numbering the trimers. The t_{ab} and U_{ab} take the values t and U for intra-, and t' and U' for inter-trimer hopping, $n_a = f_a^\dagger f_a$, and f_a is the fermionic annihilation operator. The sites in each trimer are enumerated as in Fig. 1a. We denote the 3 different intra-trimer modes by $f^{(i)} = (f_{1,i} + f_{2,i} + f_{3,i})/\sqrt{3}$ (zero momentum mode), and $f_{\pm}^{(i)} = (f_{1,i} + z_{\pm} f_{2,i} + z_{\pm}^2 f_{3,i})/\sqrt{3}$ (left and right chirality modes), where $z_{\pm} = \exp(\pm 2\pi i/3)$.

In the limit of weak coupling between the trimers of the original Kagomé lattice, the problem of two fermions per trimer (filling 2/3) becomes equivalent to a quantum magnet on a triangular lattice with couplings that depend on the bond directions as described by the Hamiltonian

$$H = \frac{J}{2} \sum_{i=1}^N \sum_{j=1}^6 s_i(\phi_{i-j}) s_j(\tilde{\phi}_{j-i}), \quad (1)$$

where N denotes number of trimers, $J = 4U'/9$, and the nearest neighbors are enumerated as in Fig. 1a. In Eq. (1) we have $s_i(\phi) = \cos(\phi) s_x^{(i)} + \sin(\phi) s_y^{(i)}$, where the spin-1/2 operators $s_x^{(i)}$, $s_y^{(i)}$ are defined as: $s_x^{(i)} =$

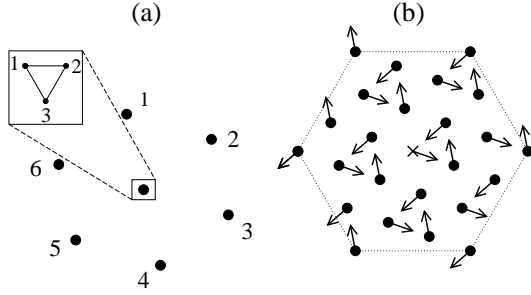


FIG. 1: (a) enumeration of inter (intra) trimer nearest neighbors; (b) classical 120° state with *left* chirality.

$(f_+^{(i)\dagger} f_-^{(i)} + f_-^{(i)\dagger} f_+^{(i)})/2$, $s_y^{(i)} = -i(f_+^{(i)\dagger} f_-^{(i)} - f_-^{(i)\dagger} f_+^{(i)})/2$. The angles ϕ are: $\phi_{i \rightarrow 1} = \phi_{i \rightarrow 6} = 0$, $\phi_{i \rightarrow 2} = \phi_{i \rightarrow 3} = 2\pi/3$, $\phi_{i \rightarrow 4} = \phi_{i \rightarrow 5} = -2\pi/3$, $\phi_{i \rightarrow 1} = \phi_{i \rightarrow 2} = -2\pi/3$, $\phi_{i \rightarrow 3} = \tilde{\phi}_{i \rightarrow 4} = 0$, $\tilde{\phi}_{i \rightarrow 5} = \phi_{i \rightarrow 6} = 2\pi/3$. This Hamiltonian has previously appeared in the context of a block-spin approach to the Heisenberg antiferromagnet on the Kagomé lattice (HAK) [11, 12]. The main purpose of that approach has been to find the origin of the exponentially large number of low-lying singlets that had been found in numerical studies of the Kagomé antiferromagnet [13, 14]. We stress that in this Letter, the Hamiltonian (1) describes *a physically feasible situation*.

Let us begin by discussing the semiclassical theory of the model (1), which describes well the large spin, S , limit. In addition to being translationally invariant, the model of Eq. (1) is invariant under the point group of order 6, $Z_6 = Z_3 \cdot Z_2$, where the generator of Z_3 (order 3) is the combined rotation of the lattice by the angle $4\pi/3$, and of the spins by the angle $2\pi/3$, while the generator of Z_2 (order 2) is the spin inversion in the $x - y$ plane, $s_j^x \rightarrow -s_j^x$, $s_j^y \rightarrow -s_j^y$. We remark that our model possesses no continuous spin rotational symmetry. There exist three ordered classical states with small unit cells that are compatible with this point-group symmetry of the model: a ferromagnetic state, and two 120° Néel type structures with left (Fig. 1b) and right (Fig. 2a) chiralities. The energies per site of these states are $E_{\text{class}}^{\text{ferro}} = E_{\text{class}}^{\text{right}} = -3S^2J/4$ and $E_{\text{class}}^{\text{left}} = 3S^2J/2$, where the subscripts “right” and “left” refer to chiralities. Hence, for $J < 0$ the state with left-handed chirality will be the ground state (GS). For $J > 0$ the situation is more complex: the states with right-handed chirality and the ferromagnetic state are degenerate ground states.

We consider first the $J > 0$ case. A spin-wave expansion around the ferromagnetic state based on the Holstein-Primakoff expansion of the spin operators is straightforward [15]. The spin-wave frequency $\omega^{\text{ferro}}(\mathbf{q}; \theta)$ depends on the direction θ of the magnetization relative to the main directions of the triangular lattice: $\omega^{\text{ferro}}(\mathbf{q}; \theta) = \frac{3}{2}JS[1 - \frac{4}{3}\sum_{i=1}^3 f_i(\mathbf{q}; \theta)]^{1/2}$, with $f_1(\mathbf{q}; \theta) = -\sin(\theta_0 + \theta)\sin\theta\cos(\mathbf{q}\delta_1)$, $f_2(\mathbf{q}; \theta) = \sin(\theta_0 + \theta)\sin(\theta_0 - \theta)\cos(\mathbf{q}\delta_2)$, and $f_3(\mathbf{q}; \theta) = \sin(\theta_0 -$

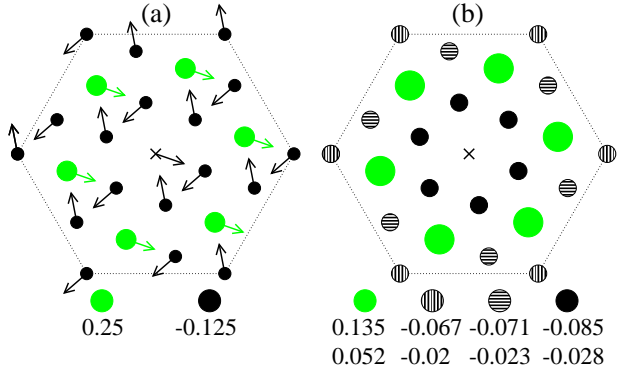


FIG. 2: (color online). (a) classical 120° state with *right* chirality. Dots show $s_x^{(i)} s_x^{(10)} + s_y^{(i)} s_y^{(10)}$, where $|\vec{s}| = 1/2$ [16]; (b) spin-spin correlations, $\langle s_x^{(i)} s_x^{(10)} + s_y^{(i)} s_y^{(10)} \rangle$. The upper [lower] set of values corresponds to $kT = 0$ [$kT = 10^{-2}J/2$]. For both plots $N = 21$ and $i = 10$ at the central site.

$\theta)\sin\theta\cos(\mathbf{q}\delta_3)$. Here, $\theta_0 = 2\pi/3$, $\delta_1 = -1/2 \mathbf{e}_x + \sqrt{3}/2 \mathbf{e}_y$, $\delta_2 = 1/2 \mathbf{e}_x + \sqrt{3}/2 \mathbf{e}_y$ and $\delta_3 = \mathbf{e}_x$ are unit vectors along three lattice directions of the triangular lattice (see Fig. 2a and [16]), and θ is the angle between the direction of the magnetization and δ_3 . The lowest order quantum correction to the classical GS energy $E_{\text{class}}^{\text{ferro}}$ is $\delta E^{\text{ferro}}(\theta) = -\frac{3}{4}JS + \frac{1}{2N}\sum_{\mathbf{q}}\omega^{\text{ferro}}(\mathbf{q}; \theta)$. It is minimal if θ takes one of the six values $\frac{\pi}{3}j$, $j = 1 \dots 6$. Thus, the first order quantum correction breaks the continuous symmetry of the classical ferromagnetic state with respect to the direction of the magnetization leaving only a sixfold degeneracy. After inclusion of the first order quantum correction, the energy of these six states becomes $E^{\text{ferro}}(S) = -\frac{3}{4}J[S(S+1) - 0.901S]$.

In obtaining the spin wave expansions around the two 120° Néel states we closely followed the method of Jolicoeur and Le Guillou [17]. The three sublattice structure of these states requires that one introduces three different Holstein-Primakoff bosons, and correspondingly one obtains three different spin-wave branches defined on the \mathbf{q} points of the reduced hexagonal Brillouin zone.

For the state with right-handed chirality all three branches are dispersionless. While the lowest branch is a branch of zero-frequency modes, the two other branches are degenerate with a constant frequency $\omega^{\text{right}} = \frac{1}{2}\sqrt{\frac{3}{2}}JS$. The zero-frequency modes correspond to rigid rotations of the three spins on the corners of the downward pointing triangles around an axis perpendicular to the spin plane. After inclusion of the lowest order quantum corrections, the GS energy of this state is $E^{\text{right}}(S) = -\frac{3}{4}J[S(S+1) - 1.48S]$. Obviously, $E^{\text{ferro}}(S) < E^{\text{right}}(S)$, i. e. the lowest order corrections to the classical ground states suggest that the ferromagnetic state is the true GS for $J > 0$.

For $J < 0$, when the GS is the state with left handed chirality, the two lower spin-wave branches are disper-

sive: $\omega_{1(2)}^{\text{left}}(\mathbf{k}) = \frac{3}{2}|J|S\sqrt{3 - (+)\sqrt{1 + 2Q(\mathbf{k})}}$, where $Q(\mathbf{k}) = 1 + \cos(3k_x/2 + \sqrt{3}k_y/2) + \cos(3k_x/2 - \sqrt{3}k_y/2) + \cos(\sqrt{3}k_y)$. The highest branch is dispersionless again:

$\omega_3^{\text{left}} = 3\sqrt{\frac{3}{2}}|J|S$. Inclusion of the zero-point energies of these modes yields $E^{\text{left}} = \frac{3}{2}J[S(S+1) - 0.935S]$ for the energy of this state.

To describe the physics of spinless fermions on a trimerised optical Kagomé lattice at filling 2/3 we need to consider the model, Eq. (1), for spin 1/2, *i.e.* in the extreme quantum limit. Questions to be answered for this case are: (i) Is the GS of the model Eq. (1) an ordered state, or is it a spin liquid either of type I, *i.e.* a state without broken symmetry, with exponentially fast decaying spin-pair correlations and a gap to the first excitation, or of type II, *i.e.* a Kagomé-like GS again without broken symmetry, with extremely short ranged correlations, but with a dense spectrum of excitations adjacent to the GS; (ii) What are the thermal properties of our system? After all, the model can only be realized at finite, albeit low temperatures.

To answer the above questions we have performed exact diagonalization of the Hamiltonian (1) for $N = 12, 15, 18, 21$, and 24 spins using the ARPACK routines [18]. To simplify the problem we used all translational symmetries of (1), and split a single diagonalization of a $2^N \times 2^N$ matrix into N independent diagonalizations of $\approx 2^N/N \times 2^N/N$ matrices. Despite all these efforts, studies of larger systems require usage of massive computer resources. Fortunately, the results for 21 and 24 spins show qualitative and quantitative resemblance, and we regard them as representative for larger systems.

Our findings are presented in Figs. 2b and 3 and Tables I and II. For $J > 0$, in contrast to the semiclassical result, the ground state exhibits the 120° Néel order with right chirality [19]. This is illustrated in Fig. 2b, where the planar spin-spin correlations are presented. Direct comparison with the correlations calculated for the classical state (Fig. 2a), shows that for the exact quantum calculation the correlations, although smaller, have the same order of magnitude and sign as in the classical case. Especially, the relative values of correlations compare nicely to the classical result: Table I summarizes the results for $N = 21$ and $N = 24$. Amazingly, the 120° Néel order survives at finite temperatures, as indicate the results obtained for $kT = 10^{-2}J/2$ and presented in Fig. 2b. At such temperatures about 800 low energy eigenstates contribute to the correlations.

For smaller systems, $N < 21$ ($J > 0$), finite size effects affect spin correlations strongly. Nevertheless, a ground state energy per spin can be reliably extracted from the data for $N \geq 12$, resulting in $-0.2175J - 0.0755J/N$.

These results support our speculation that the quantum GS of the model Eq. (1) shows 120° planar Néel order. This implies that the GS breaks the translational

	1		$\sqrt{3}$		2		$\sqrt{7}$		3	
120°	-0.125	1.0	0.25	2.0	-0.125	1.0	-0.125	1.0	0.25	2.0
$N=24$	-0.096	1.0	0.162	1.69	-0.083	0.86	-0.080	0.83	0.156	1.63
$N=21$	-0.085	1.0	0.135	1.59	-0.071	0.84	-0.067	0.79		

TABLE I: Spin correlations for $J > 0$. For every distance from a reference center ($1, \dots, 3$ in lattice units) the left most number is a planar spin-spin correlation, while the right most one is the absolute value of that correlation divided by the nearest neighbor spin correlation in the considered system.

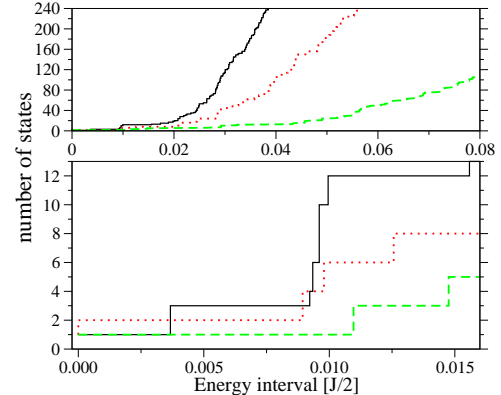


FIG. 3: (color online). Number of states in an energy interval above the GS: black (solid), red (dotted) and green (dashed) lines correspond to system's sizes 24, 21 and 18, respectively.

and the point group symmetry of our model, but there is no continuous symmetry which could be broken by this state. Therefore, the standard expectation would be that the excitations are gapped, and that the gap is of order of J . Instead, we find that the system has an exceptionally large number of low energy excitations (see Fig. 3). For instance, for $N = 21$ in the energy interval $0.1J/2$ there are about 800 excited states. All of them support the spin order of the GS so that this order persists at finite temperatures.

The analysis of the results for different N 's is compatible with an exponential increase of the number of low-energy states with the system size N similarly as in the case of the $S = 1/2$ HAK. [13, 14]. For the HAK Mila has been able to explain this high density of low energy states by associating them approximately to dimer coverings of an effective triangular lattice with uncorrelated products of nearest-neighbor pair states [12]. His method fails here, because the low-lying states of our model must certainly be highly correlated. On account of the breaking of the discrete symmetries of our model by the Néel order, one expects the ground state of the *infinite* system to be sixfold degenerate. For *finite* systems this degeneracy is lifted. Nevertheless, we expect to find six low-lying states in the gap below the lowest excited state. In view of this scenario the inspection of the lower panel of Fig. 3 suggests that the gap, if any, is smaller than $10^{-2}J/2$. The appearance of this very small energy scale is com-

	1	$\sqrt{3}$	2	$\sqrt{7}$
120°	-0.125	0.25	-0.125	-0.125
N=21	-0.134	0.237	-0.117	-0.116
N=12	-0.137	0.251	-0.125	

TABLE II: Spin-spin planar correlations for $J < 0$ as a function of distance $1, \dots, \sqrt{7}$ in lattice units.

pletely unexpected and puzzling. Obviously, the answer to the questions (i) and (ii) above, is that the GS is ordered, and that the order survives at low temperatures. The smallness of the gap and the large density of low-energy states, however, resemble very much the behavior of a quantum spin liquid of type II. For these reasons we propose to term our system a *quantum spin liquid-crystal*. We remark in this context, that the specific heat of $N = 21$ system exhibits a peak at $kT \sim 7 \cdot 10^{-3} J/2$.

The above results for $J > 0$ contrast dramatically with the results for $J < 0$, summarized in Table II. In the latter case we deal with the standard quantum antiferromagnet with 120° Néel order and left chirality [19] (Fig. 1b). The spectrum is gapped, and the semiclassical theory works remarkably well even for system sizes as small as $N = 12$. The gap is of the order $|J|/2$ in this case ($N = 12, 18, 21$), meaning that there are at most a few states with energies substantially below $|J|/2$ for $J < 0$, as opposed to the huge number for $J > 0$ (Fig. 3).

The observation of physics described in this Letter requires achieving low, but not unrealistic temperatures $\simeq 10\text{nK}$ to 100nK (c.f. Ref. [10, 20]). The low energy states may be prepared employing adiabatic changes of the degree of trimerization of the lattice. For instance one can start with a completely trimerized lattice; the filling $\nu = 2/3$ may be achieved then by starting with $\nu = 1$, and eliminating 1 atom per trimer using, for instance, laser excitations. One can then increase t and U slowly, on the time scale slower than the final $1/J$ (\simeq seconds). Alternatively, one could start with $\nu \simeq 2/3$ in the moderately trimerized regime. As in Ref. [6], the inhomogeneity of the lattice due to the trapping potential, would then allow to achieve the Mott state with $\nu = 2/3$ per trimer in the center of the trap. It should then be possible to measure the energy of the system simply by opening the lattice; by repeated measurement of the energy $E(T)$ at (definite) finite temperatures one would get in this way an access to the density of modes, i.e. could compare the results with Fig. 3. From such measurements one could infer about the existence of the gap E_{gap} , since if E_{gap} is large enough, $E(T)$ becomes T -independent for $kT \leq E_{\text{gap}}$. Various other correlations could be measured using the methods proposed in Ref. [21]. In order to measure planar spin correlations, one has, however, to lift the degeneracy of the f_{\pm} modes, e.g. by slightly modifying the intensity of one of the superlattices forming the trimerized lattice. This should be done on a time scale faster than the characteristic time scales of other inter-

actions, so that the state of the system would not change during the measurement. In such a case one can use far off resonant Raman scattering (or scattering of matter waves) to measure the dynamic structure factor, which is proportional to the spatio-temporal Fourier transform of the density-density correlations. At frequencies close to the two photon resonance of the Raman transition between the f_{\pm} modes, only $f_+ - f_-$ transitions contribute to the detected signal, and hence such measurement would yield exactly information about the spatial correlations of the type $\langle f_+^{(i)\dagger} f_-^{(i)} f_-^{(j)\dagger} f_+^{(j)} \rangle$, and hence about the planar spin correlations of Fig. 2.

A.H. is indebted to D.C. Cabra and P. Pujol for collaboration in a preliminary investigation related to the present work. We acknowledge support from the Deutsche Forschungsgemeinschaft (SFB 407, SPP1116, 436 POL), ESF Programme QUDEDIS, and the Alexander von Humboldt Foundation.

- [1] D. Jaksch *et al.*, Phys. Rev. Lett. **81**, 3108 (1998); D. Jaksch and P. Zoller, cond-mat/0410614.
- [2] L.-M. Duan, E. Demler, and M.D. Lukin, Phys. Rev. Lett. **91**, 090402 (2003).
- [3] W. Hofstetter *et al.*, Phys. Rev. Lett. **89**, 220407 (2002).
- [4] B. Damski *et al.*, Phys. Rev. Lett. **90**, 110401 (2003); A. Sanpera *et al.*, *ibid.*, **93**, 040401 (2004).
- [5] J.I. Cirac and P. Zoller, Phys. Today **57**, 37 (2004).
- [6] M. Greiner *et al.*, Nature **415**, 39 (2002).
- [7] S. Peil *et al.*, Phys. Rev. A **67**, 051603(R) (2003); J.V. Porto *et al.*, Phil. Tans. Roy. Soc. **361**, 1417 (2003).
- [8] G. Misguich and C. Lhuillier, cond-mat/0310405, to appear in “Frustrated spin systems”, edited by H.T. Diep (World-Scientific, Singapore, 2004).
- [9] L. Santos *et al.*, Phys. Rev. Lett. **93**, 030601 (2004).
- [10] H. Fehrmann *et al.*, cond-mat/0307635 (to appear in Opt. Comm. (2004)).
- [11] V. Subrahmanyam, Phys. Rev. B **52**, 1133 (1995).
- [12] F. Mila, Phys. Rev. Lett. **81**, 2356 (1998); M. Mambrini and F. Mila, Eur. Phys. J. B **17**, 651 (2000).
- [13] P. Lecheminant *et al.*, Phys. Rev. B **56**, 2521 (1997).
- [14] Ch. Waldtmann *et al.*, Eur. Phys. J. B **2**, 501 (1998).
- [15] A. Auerbach, *Interacting Electrons and Quantum Magnetism*, (Springer, New York, 1994).
- [16] Direction and position of the central spin in Fig. 1b define the x axis. The y axis points up in the figure’s plane.
- [17] Th. Jolicoeur and J.C. Le Guillou, Phys. Rev. B **40**, 2727 (1989).
- [18] <http://www.caam.rice.edu/software/ARPACK/>.
- [19] The chirality is found from $\langle s_x^{(i)} s_y^{(j)} - s_y^{(i)} s_x^{(j)} + s_x^{(j)} s_y^{(k)} - s_y^{(j)} s_x^{(k)} + s_x^{(k)} s_y^{(i)} - s_y^{(k)} s_x^{(i)} \rangle$, where i, j, k enumerate sites of the smallest triangular substructures; see S. Miyashita, Prog. Theor. Phys. Suppl. **87**, 112 (1986).
- [20] Phonon-based cooling may also be used; A.J. Daley, P.O. Fedichev, and P. Zoller, Phys. Rev. A **69**, 022306 (2004).
- [21] J.J. García-Ripoll, M.A. Martin-Delgado, and J.I. Cirac, cond-mat/0404566.